PROCEEDINGS OF SCIENCE

The Sivers asymmetry of vector meson production in semi-inclusive deep inelastic scattering

Yongjie Deng,[a,*] **Tianbo Liu**[a,b] **and Ya-jin Zhou**[a]

[a] *Key Laboratory of Particle Physics and Particle Irradiation (MOE), Institute of Frontier and Interdisciplinary Science, Shandong University, Qingdao, Shandong 266237, China*

[b] *Southern Center for Nuclear-Science Theory (SCNT), Institute of Modern Physics, Chinese Academy of Sciences, Huizhou, Guangdong 516000, China*

E-mail: yongjie.deng@mail.sdu.edu.cn, liutb@sdu.edu.cn, zhouyj@sdu.edu.cn

The transverse single spin asymmetries of ρ^0 production in semi-inclusive deep inelastic scattering (SIDIS) are recently measured by COMPASS. Among them, the Sivers asymmetry can be described by the convolution of the Sivers function and the unpolarized fragmentation function within the transverse momentum dependent factorization. We perform a phenomenological study and find that the COMPASS data can be well described by the nucleon Sivers functions extracted from previous SIDIS data with pion and kaon productions. Therefore, it provides a universality test of the nucleon Sivers functions within the current experimental precision. Based on the result, we predict the Sivers asymmetry of ρ^0 production in SIDIS at future experimental facilities, such as the electron-ion colliders. The production of other vector mesons, like K^*, is also discussed.

25th International Spin Physics Symposium (SPIN 2023)
24-29 September 2023
Durham, NC, USA

*Speaker

PoS(SPIN2023)070

1. Introduction

Understanding the internal structure of nucleons at the quark and gluon level is an important topic in modern physics. Quarks and gluons, due to the phenomenon of color confinement, cannot be directly observed. The semi-inclusive deep inelastic scattering (SIDIS) process is one of the primary tools for probing the three-dimensional structure of the nucleon. In the transverse momentum dependent (TMD) factorization framework, the cross section of the SIDIS process can be expressed as the convolution of the transverse momentum dependent parton distributions (TMD PDFs), the hard part, and the transverse momentum dependent fragmentation functions (TMD FFs). The correlations of spin and momentum in the TMD PDFs and the TMD FFs result in azimuthal angular asymmetries in the distribution of final-state hadrons. Among them, the Sivers asymmetry, a target transverse single spin asymmetry, is the most extensively measured by HERMES [1–3], COMPASS [4–10], and JLab [11, 12]. The Sivers asymmetry can be described as the convolution of the Sivers function of the target nucleon and the unpolarized fragmentation function of the final-state hadron. It is also the main observable for existing phenomenology extractions of the Sivers function. In these SIDIS experiments, the final-state hadrons are either unidentified charged hadrons or identified pions, kaons, and protons, with either 0 or $1/2$ spins.

Recently, the COMPASS Collaboration measured the Sivers asymmetry of ρ^0 [13], which is the first measurement of the Sivers asymmetry in vector meson production. According to the factorized formalism, the Sivers function of the nucleon is independent of the type of the identified hadron in the final state of the SIDIS process. Therefore, the measurement of the Sivers asymmetry of the ρ^0 meson may serve as a universality test of the Sivers function. In addition, the primary decay products of vector mesons, being pseudoscalar mesons, would also contaminate the data concerning pions and kaons. So the study of the Sivers asymmetry in vector meson productions will not only enrich our understanding of the Sivers effect in vector meson production but also in pseudoscalar mesons such as pions and kaons.

In this work, we perform a calculation of the Sivers asymmetry of the ρ^0 production at the kinematic region measured by COMPASS [13] based on our current knowledge of the Sivers function from pion and kaon data. This analysis serves as a test for the universality of the Sivers function of the nucleon. Furthermore, we present the anticipated Sivers asymmetry of ρ^0 and K^* at the kinematic regions of EIC [14, 15] and JLab22 [16]. The theoretical formalism is introduced in Sec. 2, the numerical results are presented in Sec. 3, and the summary is given in Sec. 4.

2. Theoretical formalism

For the SIDIS process where an unpolarized lepton beam scatters off a transversely polarized nucleon target, the cross section can be written in the following form,

$$\frac{\mathrm{d}\sigma}{\mathrm{d}x_B\,\mathrm{d}y\,\mathrm{d}z_h\,\mathrm{d}P_{h\perp}^2\,\mathrm{d}\phi_h\,\mathrm{d}\phi_S} \sim \left[F_{UU} + \sin\left(\phi_h - \phi_S\right) F_{UT}^{\sin(\phi_h-\phi_S)} + \ldots\right], \tag{1}$$

where $P_{h\perp}$ is the final-state hadron transverse momentum, and ϕ_h and ϕ_S are respectively the azimuthal angles of the final-state hadron and of the polarization of the target in the virtual photon-nucleon center-of-mass frame. In this work, we focus on the Sivers effect, which is associated

with F_{UU} and $F_{UT}^{\sin(\phi_h-\phi_S)}$. Other structure functions are represented with an ellipsis in Eq. (1). The Sivers asymmetry $A_{UT}^{\sin(\phi_h-\phi_S)}$ can be expressed as the ratio of the corresponding structure functions,

$$A_{UT}^{\sin(\phi_h-\phi_S)} = 2\left\langle \sin\left(\phi_h-\phi_S\right)\right\rangle = \frac{F_{UT}^{\sin(\phi_h-\phi_S)}}{F_{UU}}. \tag{2}$$

Within the TMD factorization and evolution, the structure functions can be written in the following forms,

$$F_{UT}^{\sin(\phi_h-\phi_S)}\left(x_B, z_h, P_{h\perp}, Q^2\right) = \mathcal{B}_1\left[\widetilde{f}_{1T}^{\perp}\,\widetilde{D}_1\right], \quad F_{UU}\left(x_B, z_h, P_{h\perp}, Q^2\right) = \mathcal{B}_0\left[\widetilde{f}_1\,\widetilde{D}_1\right], \tag{3}$$

where the shorthand notation $\mathcal{B}_n\left[fD\right]$ is

$$\mathcal{B}_n\left[fD\right] = \sum_q e_q^2 \int_0^\infty \frac{\mathrm{d}b}{2\pi} b^{n+1} J_n\left(\frac{bP_{h\perp}}{z_h}\right)\left(\frac{Q^2}{\zeta_Q(b)}\right)^{-2\mathcal{D}(b,Q)} f_{q/p}\left(x_B, b\right) D_{h/q}\left(z_h, b\right). \tag{4}$$

This expression is obtained by using the ζ-prescription to perform the TMD evolution. The functions $\widetilde{f}_{1,q/p}\left(x,b\right)$, $\widetilde{D}_{1,h/q}\left(z,b\right)$, and $\widetilde{f}_{1T,q/p}^{\perp}\left(x,b\right)$ are the so-called optimal unpolarized TMD PDF, the optimal unpolarized TMD FF, and the optimal Sivers function, respectively. There are two recent parametrizations of the optimal Sivers function $\widetilde{f}_{1T,q/p}^{\perp}\left(x,b\right)$, the BPV20 parametrization [17] and the ZLSZ parametrization [18]. In our calculation, we use 500 replicas of the BPV20 parametrization and 100 replicas of the ZLSZ parametrization. For the optimal unpolarized TMD PDF $\widetilde{f}_{1,q/p}\left(x,b\right)$, we adopt the parametrization in Ref. [19].

We obtain the optimal unpolarized TMD FF $\widetilde{D}_{1,h/q}\left(z,b\right)$ by following the approach in Ref. [19]. In the small b region where the perturbative approximation is good, the optimal unpolarized TMD FF $\widetilde{D}_{1,h/q}\left(z,b\right)$ should be matched to the collinear functions as

$$\widetilde{D}_{1,h/f}\left(z,b\right) = \frac{1}{z^2}\sum_{f'}\int_z^1 \frac{\mathrm{d}y}{y} y^2 \mathbb{C}_{f\to f'}\left(y, b, \mu_{\mathrm{OPE}}^{\mathrm{FF}}\right) D_{1,h/f'}\left(\frac{z}{y}, \mu_{\mathrm{OPE}}^{\mathrm{FF}}\right) D_{\mathrm{NP}}\left(z,b\right), \tag{5}$$

where the coefficient functions $\mathbb{C}_{f\to f'}$ are the Wilson coefficients. The scale $\mu_{\mathrm{OPE}}^{\mathrm{FF}}$ is chosen as

$$\mu_{\mathrm{OPE}}^{\mathrm{FF}} = \frac{2e^{-\gamma_E} z_h}{b} + 2\,\mathrm{GeV}. \tag{6}$$

$D_{1,h/f'}\left(z,\mu\right)$ represents the collinear FF. Up to now there is no appropriate parametrization available for the collinear FF of ρ^0 meson. To find a reasonable parametrization we perform a fit to the Pythia data on ρ^0 meson production using the following parametrization form,

$$D_{h/i}\left(z, Q_0^2\right) = N_i^h z^{\alpha_i^h}\left(1-z\right)^{\beta_i^h}, \quad \left(i = u, d, s, g, \bar{u}, \bar{d}, \bar{s}\right). \tag{7}$$

The parameters in this form are listed in Table 1.

For the $D_{\mathrm{NP}}\left(z,b\right)$, which characterize the nonperturbative TMD effect, we assume the function form for the ρ^0 meson as those parametrized for pion and kaon [19],

$$D_{\mathrm{NP}}\left(z,b\right) = \exp\left[-\frac{\eta_1 z + \eta_2(1-z)}{\sqrt{1+\eta_3(b/z)^2}}\frac{b^2}{z^2}\right]\left(1+\eta_4\frac{b^2}{z^2}\right), \tag{8}$$

function	N	α	β
$D_{\rho^0/u} = D_{\rho^0/\bar{u}} = D_{\rho^0/d} = D_{\rho^0/\bar{d}}$	0.4224 ± 0.0013	-0.6119 ± 0.0035	1.2448 ± 0.0037
$D_{\rho^0/s} = D_{\rho^0/\bar{s}}$	0.3346 ± 0.0044	-0.7777 ± 0.0127	2.0681 ± 0.0229
$D_{\rho^0/g}$	129.04 ± 21.159	3.2234 ± 1.6011	9.9508 ± 8.5609

Table 1: Parameters determined for ρ^0

and adopt three sets of η values in the numerical calculation, where the first set, labeled by 'scenario 1', is the same with pion and kaon ($\eta_1 = 0.260$, $\eta_2 = 0.476$, $\eta_3 = 0.478$, and $\eta_4 = 0.483$), and in 'scenario 2' ('scenario 3') all the η values are multiplied by a factor 0.3 (3). The TMD FF with these three scenarios of $D_{\rm NP}$ exhibit different transverse momentum distributions, to show this we displays the TMD FF of the ρ^0 meson as a function of $p_\perp$ for these three $D_{\rm NP}$ scenarios in Fig. 1, with $z = 0.4$, $\mu^2 = 4\,{\rm GeV}^2$. One can easily tell that with scenario 2 the TMD FF has the most concentrated $p_\perp$ distribution, followed by scenario 1, and scenario 3 displays the most diffuse $p_\perp$ distribution.

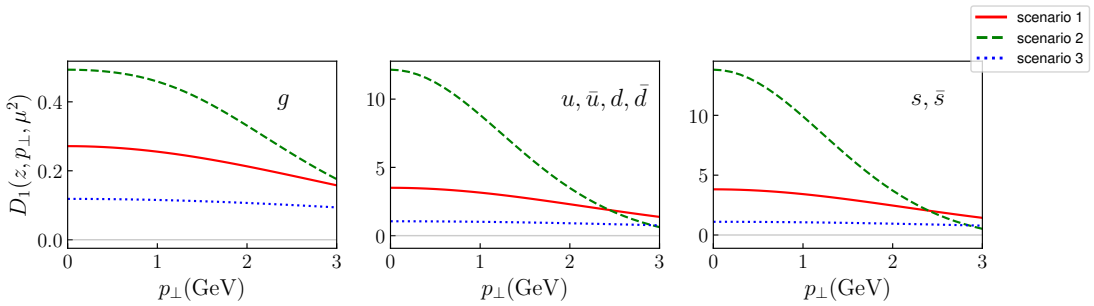

Figure 1: These three $D_{\rm NP}$ correspond to the transverse momentum distributions at $z = 0.1$, $\mu^2 = 4\,{\rm GeV}^2$.

3. Results

3.1 Sivers asymmetry of ρ^0 at the kinematic region of COMPASS

The numerical results for the Sivers asymmetry of ρ^0 at the kinematic region of COMPASS are shown in Fig 2. According to the requirements of the TMD factorization, only the data points that meet the condition $P_{h\perp}/(z_h Q) < 0.8$ are chosen.

In Fig. 2, the x_B-, z_h- and $P_{h\perp}-$dependent Sivers asymmetries are depicted in the left, central, and right panels of the figure, respectively. The red squares with error bars represent data points from COMPASS. The solid, dashed, and dotted curves correspond to the results with scenarios 1, 2, and 3, respectively. The bands with hatches represent the corresponding 1-σ uncertainties from the Sivers functions. The upper and lower panels present the results corresponding to the ZLSZ parametrization and the BPV20 parametrization, respectively. From Fig. 2, it is evident that the numerical results obtained with both parametrizations are above zero and align well with the data of COMPASS. For ρ^0 meson, a more concentrated $k_\perp$ distribution of FF corresponds to a larger Sivers effect. However, the trends in results using these two parametrizations differ, particularly

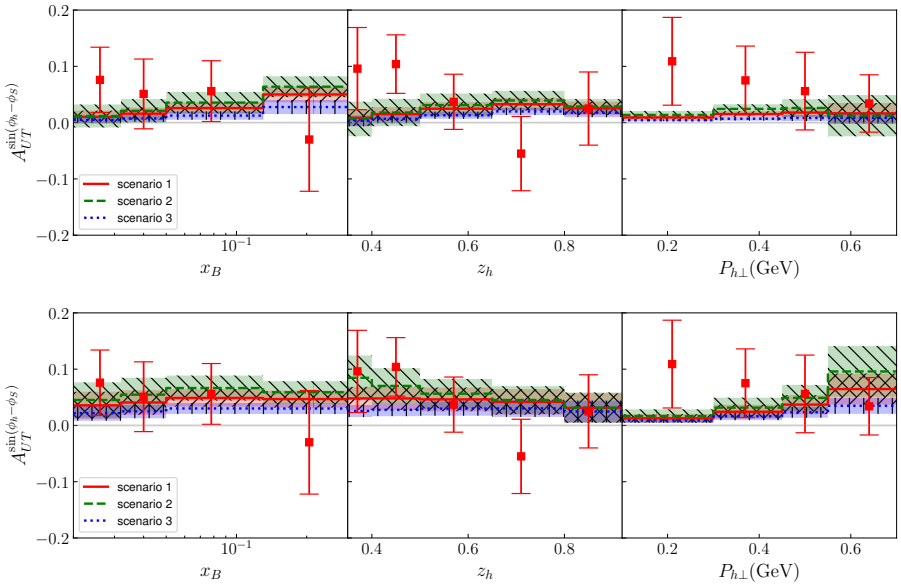

Figure 2: The numerical results of Sivers asymmetry are compared with the COMPASS measurement [13] for ρ^0 production. The upper panel presents the results using the ZLSZ parametrization [18], and the lower panel shows the results using the BPV20 parametrization [17]. The red squares with error bars represent data points from COMPASS. The bands with hatches represent the corresponding 1-σ confidence intervals.

in z_h- panel. In terms of z_h-dependence, the result obtained with the BPV20 parametrization exhibits a trend wherein a smaller z_h value corresponds to a larger Sivers asymmetry. In contrast, the ZLSZ parametrization does not show such a trend. In the Sivers asymmetry formula, the fragmentation function and the Sivers function are convolved in momentum space. The Sivers function influences the weights of different transverse momenta of the fragmentation function during the convolution. Consequently, changes in the Sivers function also impact the z_h-dependence of the Sivers effect. Furthermore, the $P_{h\perp}$-dependences of results obtained with these two parametrizations are consistent, where a larger $P_{h\perp}$ value corresponds to a larger Sivers asymmetry in both cases. The Sivers functions in both of these parametrizations are extracted from the data of pions and kaons. Our results show that the numerical calculations using these two parametrizations are both in agreement with the data of ρ^0 meson. This serves as a test for the universality of the Sivers function within the current experimental precision. Further studies require additional data. In the future, the EIC and JLab22 will play a crucial role in investigating the Sivers asymmetry of vector mesons.

3.2 The expectations of $A_{UT}^{\sin(\phi_h-\phi_S)}$ of vector mesons at the kinematic regions of EIC and JLab22

The expectations of Sivers asymmetry of ρ^0 meson at the kinematic regions of EIC and JLab22 are depicted in Fig. 3 and 4, respectively. In Figs. 3 and 4, the upper and lower panels display results obtained using BPV20 and ZLSZ parametrizations, respectively. The solid, dashed, and dotted lines correspond to scenarios 1, 2, and 3, respectively. As illustrated in Figs. 3 and 4, the expectations of Sivers asymmetry are predominantly positive, and the trends for both parametrizations align

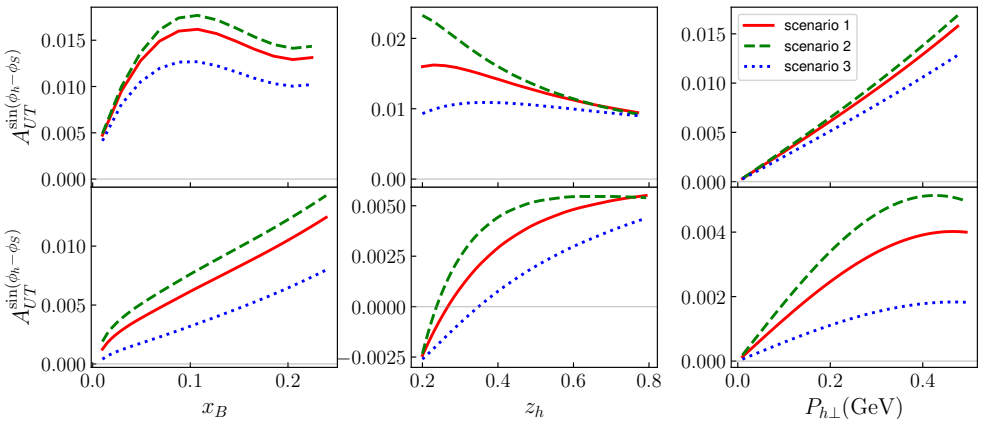

Figure 3: The anticipated Sivers asymmetry of ρ^0 meson at the kinematic region of EIC. The upper panel represents the results using BPV20 parametrization. The lower panel shows the results using ZLSZ parametrization.

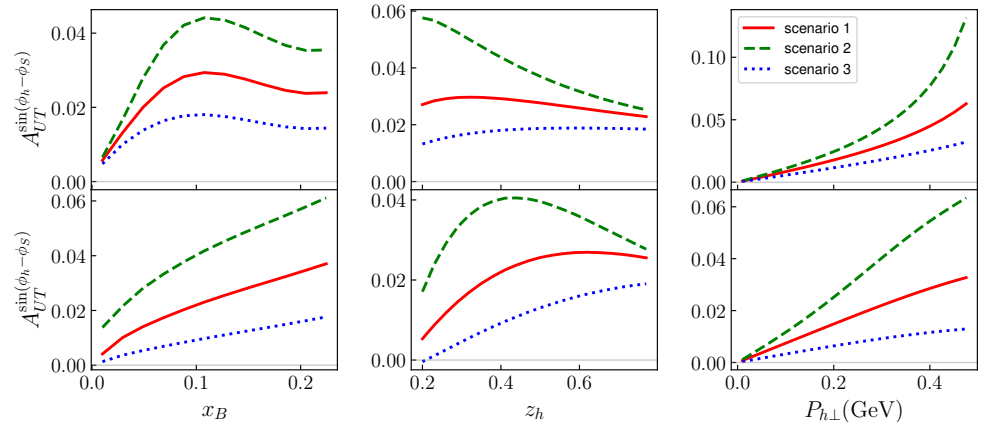

Figure 4: The anticipated Sivers asymmetry of ρ^0 meson at the kinematic region of JLab22. The upper panel represents the results using BPV20 parametrization. The lower panel shows the results using ZLSZ parametrization.

with those observed at the kinematic region of COMPASS. In Figs. 2, 3, and 4, it is evident that the scenario 2 corresponds to the most significant Sivers asymmetry. This tells us that the more concentrated the $p_\perp$ distribution of the fragmentation function, the more significant the Sivers asymmetry for ρ^0 meson. Comparing Figs. 3 and 4, it is found that there is a more significant Sivers effect at the kinematic region of JLab22 than at the kinematic region of EIC.

Additionally, the expectations of K^{*+} and $\bar{K}^{*0}$ are obtained. The K^* mesons are the vector mesons whose main decay channel is K meson and π meson. To evaluate the Sivers effect of the K^* mesons at the kinematic regions of EIC and JLab22, we follow the FFs of K^* mesons in Ref. [20]. The results of the Sivers asymmetry of K^* mesons are presented in Figs. 5, 6, 7, and 8.

Figs. 5 and 6 show the results with BPV20 parametrization and with ZLSZ parametrization at

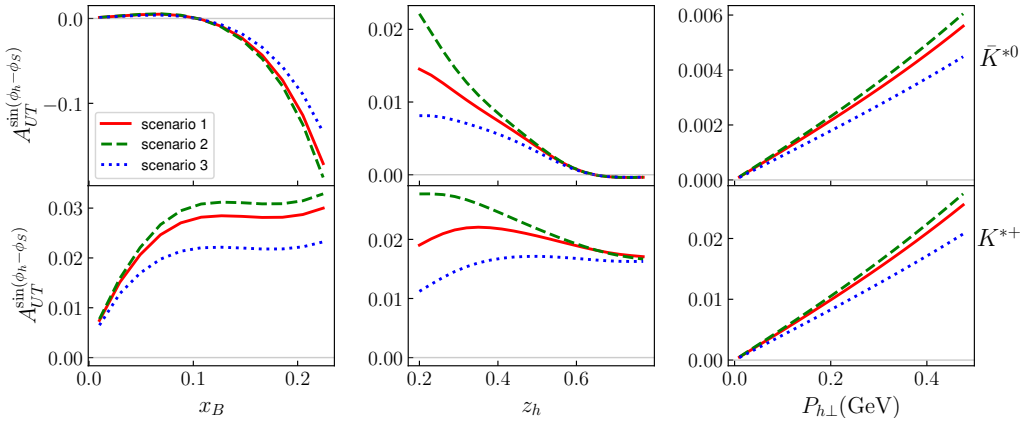

Figure 5: The expectations of K^* mesons with BPV20 parametrization at the kinematic region of EIC.

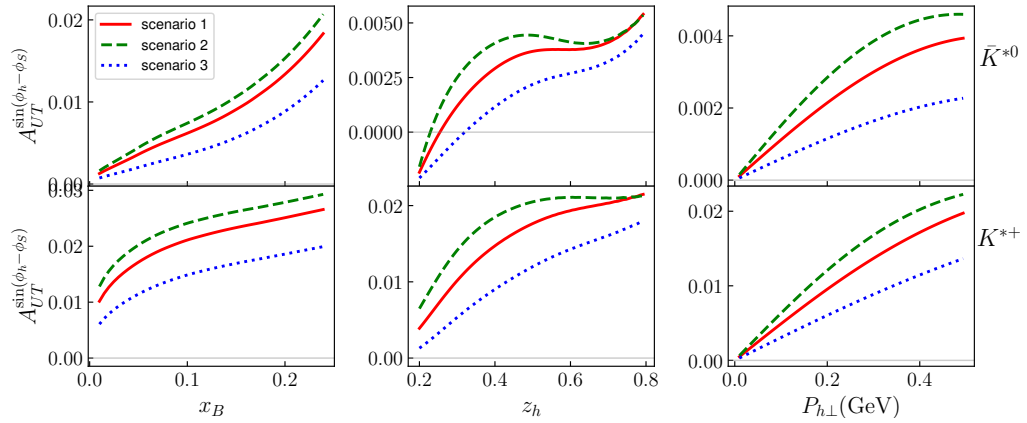

Figure 6: The expectations of K^* mesons with ZLSZ parametrization at the kinematic region of EIC.

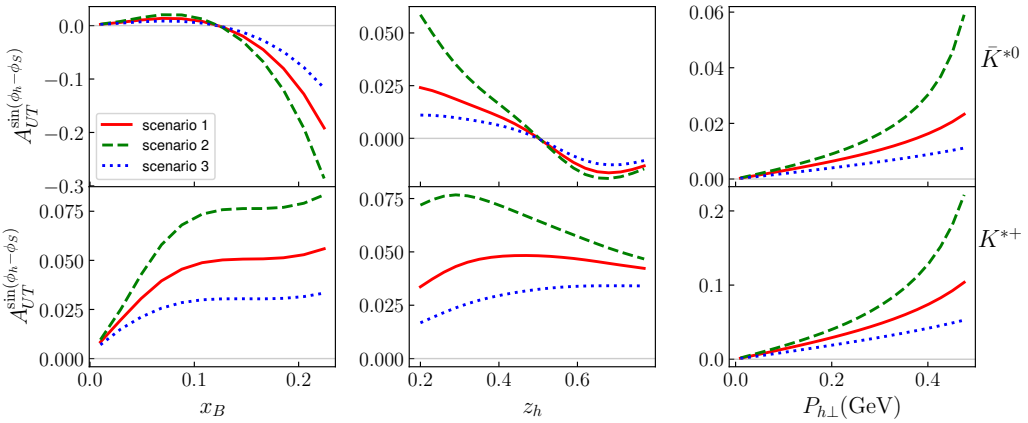

Figure 7: The expectations of K^* mesons with BPV20 parametrization at the kinematic region of JLab22.

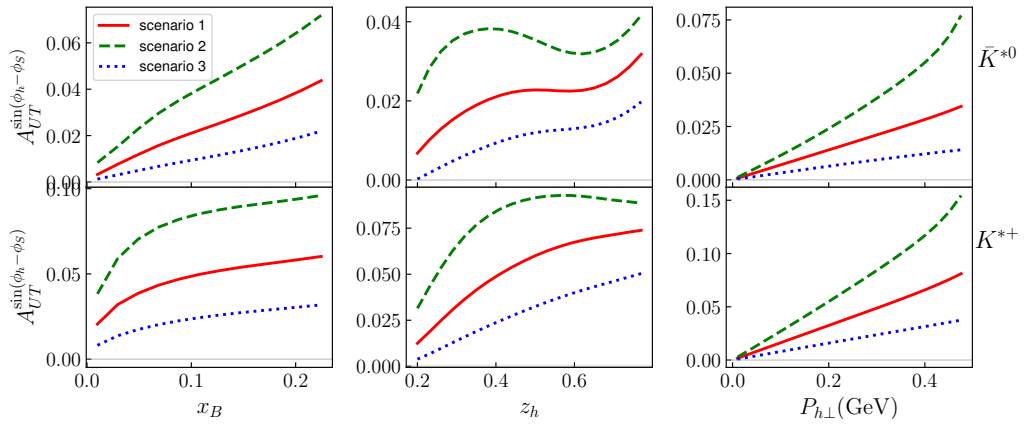

Figure 8: The expectations of K^* mesons with ZLSZ parametrization at the kinematic region of JLab22.

the kinematic region of EIC, respectively. Figs. 7 and 8 show the results with BPV20 parametrization and with ZLSZ parametrization at the kinematic region of JLab22, respectively. Like ρ^0 meson, for K^* meson, a more concentrated $p_\perp$ distribution corresponds to a more significant Sivers effect. Furthermore, from Figs. 5, 6, 7 and 8, it can be observed that there is a significant difference in the expectations with these two parametrizations at the kinematic regions of EIC and JLab22. Consequently, the Sivers effect of K^* mesons production in the SIDIS process can refine the extraction of the Sivers function.

4. Summary

We present a study of the Sivers asymmetry of the vector mesons ρ^0 and K^*. Comparing with the recent measurement by COMPASS, the numerical results are consistent with data, which serves as a test of the universality of the Sivers function. Because of the large uncertainties of the existing data and the precision of extracted Sivers functions from pion and kaon data, two recent parametrizations of the Sivers functions, the BPV20 and the ZLSZ, can both describe the COMPASS data.

The expectations of Sivers asymmetry of ρ^0 and K^* at the kinematic regions of EIC and JLab22 show a significant difference between the BPV20 parametrization and the ZLSZ parametrization. The difference between these two parametrizations offers an opportunity for further testing the universality of the Sivers function, and refining the extraction of the Sivers function. For both parametrizations, the expected values of Sivers asymmetry of ρ^0 and K^* at the kinematic region of JLab22 are relatively larger than those at the kinematic region of EIC. The next-generation colliders can provide data with much high statistical precision for the production of vector mesons, thereby advancing the research on the Sivers asymmetry of vector mesons.

Acknowledgments

We thank Zhe Zhang, Jing Zhao, and Xiaoyan Zhao for useful discussions. This work is supported by the National Natural Science Foundation of China (Grants No. 12175117 and No.

12321005) and Shandong Province Natural Science Foundation (Grants No. ZR2020MA098 and No. ZFJH202303).

References

[1] HERMES collaboration, *Single-spin asymmetries in semi-inclusive deep-inelastic scattering on a transversely polarized hydrogen target*, *Phys. Rev. Lett.* **94** (2005) 012002 [hep-ex/0408013].

[2] HERMES collaboration, *Observation of the Naive-T-odd Sivers Effect in Deep-Inelastic Scattering*, *Phys. Rev. Lett.* **103** (2009) 152002 [0906.3918].

[3] HERMES collaboration, *Azimuthal single- and double-spin asymmetries in semi-inclusive deep-inelastic lepton scattering by transversely polarized protons*, *JHEP* **12** (2020) 010 [2007.07755].

[4] COMPASS collaboration, *First measurement of the transverse spin asymmetries of the deuteron in semi-inclusive deep inelastic scattering*, *Phys. Rev. Lett.* **94** (2005) 202002 [hep-ex/0503002].

[5] COMPASS collaboration, *Sivers asymmetry extracted in SIDIS at the hard scales of the Drell–Yan process at COMPASS*, *Phys. Lett. B* **770** (2017) 138 [1609.07374].

[6] COMPASS collaboration, *Collins and Sivers asymmetries for pions and kaons in muon-deuteron DIS*, *Phys. Lett. B* **673** (2009) 127 [0802.2160].

[7] COMPASS collaboration, *II – Experimental investigation of transverse spin asymmetries in μ -p SIDIS processes: Sivers asymmetries*, *Phys. Lett. B* **717** (2012) 383 [1205.5122].

[8] COMPASS collaboration, *Measurement of the Collins and Sivers asymmetries on transversely polarised protons*, *Phys. Lett. B* **692** (2010) 240 [1005.5609].

[9] COMPASS collaboration, *A New measurement of the Collins and Sivers asymmetries on a transversely polarised deuteron target*, *Nucl. Phys. B* **765** (2007) 31 [hep-ex/0610068].

[10] COMPASS collaboration, *Measurement of P_T-weighted Sivers asymmetries in leptoproduction of hadrons*, *Nucl. Phys. B* **940** (2019) 34 [1809.02936].

[11] Jefferson Lab Hall A collaboration, *Single Spin Asymmetries in Charged Pion Production from Semi-Inclusive Deep Inelastic Scattering on a Transversely Polarized ^{3}He Target*, *Phys. Rev. Lett.* **107** (2011) 072003 [1106.0363].

[12] Jefferson Lab Hall A collaboration, *Single spin asymmetries in charged kaon production from semi-inclusive deep inelastic scattering on a transversely polarized ^{3}He target*, *Phys. Rev. C* **90** (2014) 055201 [1404.7204].

[13] G.D. Alexeev et al., *Collins and Sivers transverse-spin asymmetries in inclusive muoproduction of $\rho 0$ mesons*, *Phys. Lett. B* **843** (2023) 137950 [2211.00093].

[14] A. Accardi et al., *Electron Ion Collider: The Next QCD Frontier: Understanding the glue that binds us all*, *Eur. Phys. J. A* **52** (2016) 268 [1212.1701].

[15] R. Abdul Khalek et al., *Science Requirements and Detector Concepts for the Electron-Ion Collider: EIC Yellow Report*, *Nucl. Phys. A* **1026** (2022) 122447 [2103.05419].

[16] A. Accardi et al., *Strong Interaction Physics at the Luminosity Frontier with 22 GeV Electrons at Jefferson Lab*, 2306.09360.

[17] M. Bury, A. Prokudin and A. Vladimirov, *Extraction of the Sivers function from SIDIS, Drell-Yan, and $W^{\pm}/Z$ boson production data with TMD evolution*, *JHEP* **05** (2021) 151 [2103.03270].

[18] C. Zeng, T. Liu, P. Sun and Y. Zhao, *Toward three-dimensional nucleon structures at the Electron-Ion Collider in China: A study of the Sivers function*, *Phys. Rev. D* **106** (2022) 094039 [2208.14620].

[19] I. Scimemi and A. Vladimirov, *Non-perturbative structure of semi-inclusive deep-inelastic and Drell-Yan scattering at small transverse momentum*, *JHEP* **06** (2020) 137 [1912.06532].

[20] K.-b. Chen, Z.-t. Liang, Y.-k. Song and S.-y. Wei, *Spin alignment of vector mesons in high energy pp collisions*, *Phys. Rev. D* **102** (2020) 034001 [2002.09890].